ELSEVIER

Journal of Crystal Growth 197 (1999) 733–742

JOURNAL OF CRYSTAL GROWTH

Materials aspects of CdTe/CdS solar cells

K. Durose*, P.R. Edwards, D.P. Halliday

Department of Physics, University of Durham, South Rd., Durham DH1 3LE, UK

Abstract

The current state of CdTe/CdS solar cell development is reviewed with emphasis on the understanding of the materials behaviour. Metallurgical and optoelectronic changes effected by the $CdCl_2$ treatment are described with reference to the CdS–$CdCl_2$ and CdTe–$CdCl_2$ phase diagrams. Some studies relating to the nature, distribution and influence of important optoelectronic centres are described and some new results presented. These include PL, EBIC and CL. The potential for complex interaction of processing steps in the materials system is noted and key areas for future studies are highlighted.

1. Introduction

The current high level of research and development of the thin-film polycrystalline CdTe/CdS solar cell is driven by the possibility of producing photovoltaic modules more cheaply than ever before. Indeed two European companies are likely to be producing modules with 10 MW_p (peak power) per annum within several years. Existing CdTe technologies will be used and the target price of ECU1/watt (compared to ECU10 for crystalline silicon) will be met by using mass production techniques.

As CdTe has a near optimal band gap (1.45 eV) for solar absorption, may be doped n- or p-type and has high (direct) optical absorption above the band gap ($>10^4$ cm^{-1}), it was recognised early on as a good solar cell absorber layer (see Ref. [1]). However, homojunction devices are impractical since most absorption of the solar spectrum occurs within 1–2 μm of the CdTe surface and this makes the surface recombination loss unacceptably high. To avoid this the p-CdTe/n-CdS/TCO/glass "superstrate" configuration shown in Fig. 1 was developed [2]. The n-CdS ($E_g = 2.42$ eV) forms one side of the electrical junction and acts as a window layer. Fig. 2 shows a calculated carrier generation profile in a CdTe/CdS structure resulting from illumination by the AM1.5 solar spectrum. (AM1.5 data from Ref. [3], CdS and CdTe absorption data from [4,5].) Carriers generated in the CdTe are likely to be collected and contribute to the photocurrent, while those in the CdS are lost. Thin CdS, 50–100 nm, is therefore preferred to allow

* Corresponding author. Fax: + 44 191 374 7358; e-mail: ken.durose@durham.ac.uk.

0022-0248/99/$ – see front matter
PII: S0022-0248(98)00962-2

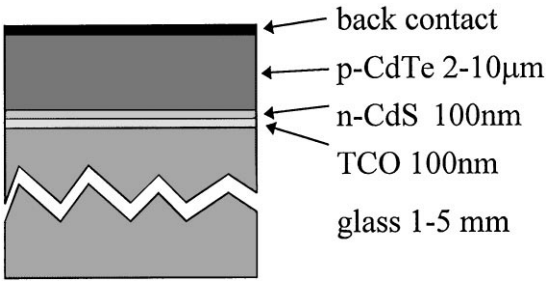

Fig. 1. The 'superstrate' configuration used for CdTe/CdS heterojunction solar cells.

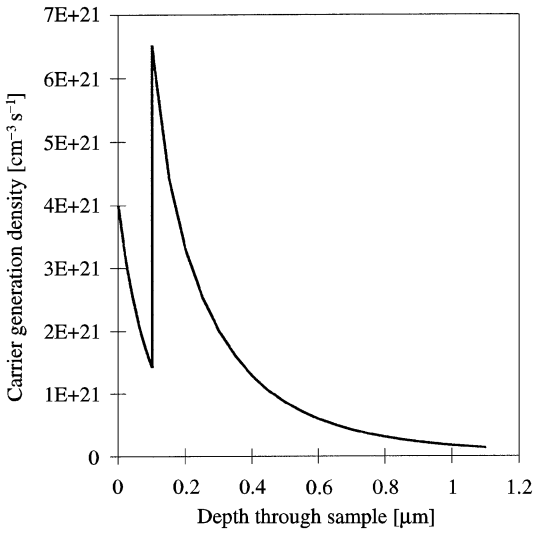

Fig. 2. Simulated profile of carriers generated in a CdTe/CdS heterostructure by AM1.5 sunlight.

above-gap optical transmission. The CdTe need only be 1–2 μm thick, but may be thicker to ensure homogeneity. Cells fabricated in this materials system are remarkably tolerant to the deposition methods used (Birkmire provides a very readable review [6]). However, the majority of cells, and *all* those with notable conversion efficiencies, were subjected to a post-growth treatment of the CdTe. Variations of the process are many but this so called "activation" or "type conversion" process usually involves annealing in the presence of $CdCl_2$. This results in an order of magnitude increase in the conversion efficiency (η) and improvements in the open circuit voltage (V_{oc}) and short

Table 1
Working parameters of CSS CdTe/CdS cells in the as-grown, annealed (400°C for 30 min in air) and $CdCl_2$ treated (i.e. coated with $CdCl_2$ then annealed) states. From Ref. [9]

Processing	V_{oc} (mV)	J_{sc} (mA cm^{-2})	FF (%)	η (%)
As deposited	0.55	6	39	1.6
Annealed	0.55	15	39	3.6
$CdCl_2$ treated	0.68	26.7	56.7	10

circuit current (J_{sc}), as has been reported by many authors (see Table 1). The maximum efficiencies reported to date are 15.8% in 1993 and 16.0% in 1998 [7,8]: advances have slowed in recent years.

Study of cells fabricated with the $CdCl_2$ methods have revealed a wealth of detail. It is considered that the $CdCl_2$ treatment effects the conversion of the CdTe from n- to p-type [10] ($p \sim 10^{14}$ cm^{-3}), lowers series resistance (e.g. 150–7 Ω cm^{-2} [11]) and is accompanied by a change in current transport mechanism from tunnelling/interface recombination to recombination in the depletion region [12]. Associated physical effects are recrystallisation [13,14], grain growth [15], and interdiffusion at the CdTe/CdS interface [16].

Although the maximum efficiency of the cells has been estimated to be over 29% [17], the best reported to date fall some way short of that. Progress in the field has been made by empiricism and recipe optimisation. Future enhancement of the performance of what is soon to be an industrial product will require progress in genuine scientific understanding.

Issues which are notable and on which progress is being made are:

(1) The means by which the $CdCl_2$ type conversion and related effects occur.

(2) The importance of grain boundaries and interfaces.

(3) The formation of conductive contacts with low barriers to p-CdTe.

An obstacle to the advancement of scientific and empirical progression of this understanding arises from the polycrystallinity of this device. All steps in the fabrication have the opportunity to influence one-another. For example the application of a back contact to the CdTe can influence the junction

region PL even if the absorber is 10 μm thick [18]. Such interdependencies make the effects of the different processing steps difficult to deconvolute.

In the next section some important aspects of the cell's layers and interfaces will be reviewed.

2. Layers and interfaces of the (contact)/CdTe/CdS/TCO solar cell

2.1. TCO, CdS and the CdS/TCO interface

2.1.1. Transparent conducting oxide

The function of the transparent conducting oxide (TCO) coated glass substrate is to provide a highly transparent and conductive contact to the CdS window layer. Sheet resistance of 5–10 Ω/□ and optical transmission over the visible range of >90% are desirable. Both SnO_2 and In_2O_3-SnO_2 (ITO) have been used successfully, but the latter is sometimes avoided to rule out diffusion of In. Multilayers such as SnO_2/ITO are sometimes used. Gerhardinger [19] points out that PV quality TCO's are produced at a rate of 0.5×10^6 m^2 per annum by CVD on float glass lines (architectural glazing products are produced in even higher volumes). Many research labs prefer to work with optimised TCO products produced in-house in small volume. For example Britt's 15.8% cell [7] was produced on MOCVD SnO_2 while Aramoto's 16.0% device [8] was deposited on sputtered ITO. At the present time the TCO is not considered to be the most problematic aspect of the cell.

2.1.2. CdS window layer

The n-CdS window layer is an essential component of the cell and although p-CdTe/TCO junctions with $\eta > 10\%$ have been demonstrated [20], that junction is fundamentally inferior. Requirements of the CdS are that it should be conductive ($n \sim 10^{16}$ cm^{-3}), thin to allow high transmission (50–100 nm) and uniform to avoid short circuit effects. Techniques used to deposit it include physical vapour deposition (PVD), MOCVD [8], close space sublimation (CSS) [21], bath plating and, for thick films, screen printing.

Chemical bath plating [22] is in most widespread use. It is a wet chemical method based on the slow, controlled decomposition of thiourea in alkaline solution and the presence of Cd^{2+} ions. Kaur's original work used cadmium acetate and the reaction proceeds in aqueous solution as follows:

$$Cd(CH_3COO)_2 + (NH_2)_2C{=}S + 2OH^- \rightarrow CdS(s) + H_2CN_2 + 2H_2O + 2CH_3COO^-.$$

The reaction proceeds heterogeneously on an immersed substrate at 90°C. There are many variations of the bath chemistry and treatment concentrations which influence the purity and physical form of the deposit. The BP group [23,24] report RBS studies showing a 10–20% excess of Cd over S which is attributed to the presence of $Cd(OH)_2$ and CdO. Kylner [25] further reports FTIR showing O–H and C≡N to be present. Some control over these impurities can be gained from varying the bath chemistry, but post-deposition treatments are often used prior to deposition of the CdTe. Heating (in air) eliminates water from $Cd(OH)_2$ to give CdO.

There is a growing literature on the intermediate use of $CdCl_2$ on the CdS to recrystallise it and enhance the n-conductivity. Such treatments probably have their origin in the processing of CdS photoconductors and were also used extensively in the sintering of screen printed CdS for solar cells. For example Lee [26] reports that sintering of CdS with 9% $CdCl_2$ effected sintering at 700°C but $CdCl_2$ segregated at the grain boundaries. This can be understood from the pseudobinary phase diagram (Fig. 3) which is of the simple eutectic type. On the CdS-rich side the last compositions to freeze are CdS and the eutectic composition. Less severe $CdCl_2$ treatments have been used to treat the CdS and have been shown effective in limiting subsequent CdTe–CdS interdiffusion [27].

2.1.3. CdS/TCO interface

The CdS/TCO interface is not considered to be an efficiency limiting one at present and consequently has been little studied. Niles [28] studies the CdS/SnO_2 interface by soft XPS. The study concluded that CdS and SnO_2 do not interdiffuse at 400°C and that the conduction band minima coincide exactly, making SnO_2 a good contact to

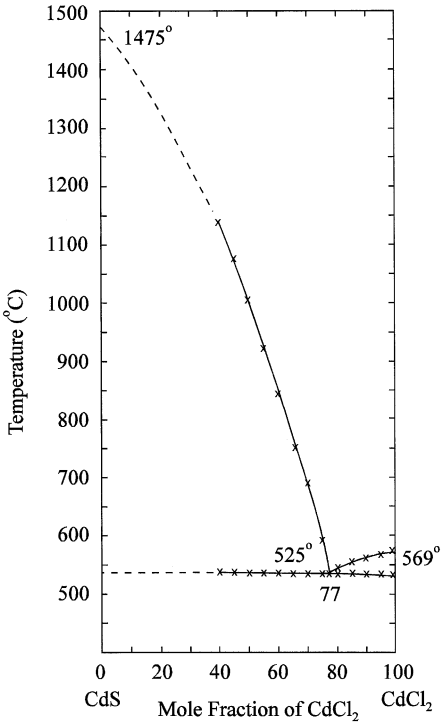

Fig. 3. Pseudobinary phase diagram for CdS–$CdCl_2$. Redrawn from Ref. [61].

n-CdS. Feng [29] on the other hand concluded that intermixing, or at least roughening, takes place and that it is beneficial in reducing reflection losses.

2.2. The CdTe absorber and the $CdCl_2$ treatment step

Aspects of the CdTe absorber layer are perhaps the most widely studied topic in the CdTe/CdS solar cell literature. As mentioned in the introduction a wide range of deposition methods has been used for CdTe including close-space sublimation (CSS) [21], screen printing [30], electrochemical [31] and MOCVD [32]. $CdCl_2$ treatment of CdTe solar cells probably had its origins both in the sintering of screen printed layers and in electrochemical deposition [10]. However, $CdCl_2$ was in use much earlier as a solvent for the solution growth of CdTe [33]. Its use in electrochemically grown material arises from the inclusion of Cl^- in the plating bath. Two main methods are used for introducing $CdCl_2$ into layers fabricated by other means. In the first the $CdCl_2$ is applied to the CdTe surface as a layer either by dip coating in $CdCl_2$/methanol solution or directly by PVD. Layers of 60–100 nm are used and annealing is typically done at 400°C for 25 min. In the second the CdTe is exposed to $CdCl_2$ vapour at the annealing temperature.

2.2.1. Metallurgical effects

The treatment is known to cause recrystallisation and grain growth in the CdTe and these effects have been the subject of several specific studies. In the as-grown state vapour deposited CdTe layers are found by TEM to be typically columnar for lower growth temperatures [6] although at high temperatures interlocking jumbles of grains of the type shown by Loginov [9] sometimes result. Although columnar growth may be considered favourable for current transport through the film, the lower temperature of growth does seem to favour twinning parallel to the interface, and this may influence transport adversely. Qi [15] studied the kinetics of grain growth in electrochemically deposited films, i.e. with the chloride ions present in the plating bath. The time dependent growth was compared to the ideal case described by Burke and Turnbull's parabolic grain growth law [34], i.e. $(D^2 - D_0^2)^{1/2} = kt^{1/n}$, where $D^2 - D_0^2$ is the difference of the squares of the average grain sizes before and after growth for a time t. k is a constant and n, the grain growth exponent, is ideally 2 above half the melting temperature. For the experiments Qi reports $n > 2$ at $350 < T < 385$°C and this is attributed to deviation from ideality, i.e. nonuniform grain boundary energies, the grains being large compared to the film thickness (columnar growth) and recrystallisation effects. Moutinho [14] points out that grain growth is not universally observed upon $CdCl_2$ treatment, especially in films with larger grains.

Recrystallisation is well known to accompany the $CdCl_2$ treatment and is frequently monitored by θ–2θ X-ray diffractometry. While as-grown films are generally reported as having the {1 1 1} preferred orientation – see Moutinho [13] for example – $CdCl_2$ treatment causes textural randomisation.

Using XRD monitoring Kim [35] derived a thermal activation energy of $E_a = 2.5 \pm 0.3$ eV for the recrystallisation and compares it to that for Cd diffusion (2.44–2.67 eV). Prolonged annealing has been reported as re-introducing the texture [35].

Moutinho [14] used AFM to monitor the recrystallisation promoted by the surface treatment method at different annealing temperatures. Recrystallisation was considered to be nucleated at the free surface with small new grains appearing at the grain interstices. Growth of these with random orientation was considered to effect the recrystallisation itself.

With regard to the mechanism of grain growth Qi [15] remarks that the parabolic law is generally obeyed at temperatures above half the melting point, in this case that of CdTe at 1091°C. It is however helpful to refer to the phase diagram for CdTe–$CdCl_2$ [36,37] in which there is a eutectic composition of 77% $CdCl_2$ and a eutectic line at 508°C. Molten material will be present above this temperature. Clearly the case of a $CdCl_2$ coated CdTe film is far from being homogeneous or at equilibrium. The diagram also indicates that the grain boundaries in $CdCl_2$ treated material will be $CdCl_2$ rich. Of course this supposes that there is complete insolubility of $CdCl_2$ in CdTe (as indicated by the diagram), but in the case of slight mutual solubility the predicted segregation provides a basis for postulating a gradient of electrically active species near the grain boundaries. This is of relevance to the model of band bending at grain boundaries mentioned in the next section.

Finally it is also commonly reported that $CdCl_2$ treatment causes smoothing of the CdTe surface [38] and the formation of deep crevasses at the grain boundaries [6]. The latter of these effects may influence contacting.

2.2.2. Opto-electronic effects

Current transport studies, that is temperature dependent I–V analysis of cells, before and after $CdCl_2$ treatment indicate a change in the current transport mechanism. In the as-grown or air annealed state transport is by tunnelling/interface recombination while afterwards it is dominated by junction recombination [11,39]. This suggests a decrease in the density of interfacial states. Some authors [39] ascribe the effect at least partly to the reduction in the volume fraction of material influenced by grain boundaries due to grain growth.

Laurenço [40] has recently undertaken a DLTS study of CSS CdTe/CdS cells which had been annealed with $CdCl_2$ layers of varying thickness (0–120 nm). A stable hole trap was observed in all samples but its activation energy decreased smoothly (from 484 ± 4 to 195 ± 7 meV) with the increasing severity of the $CdCl_2$ treatment. This was accompanied by an increase in capture cross section from 2.6×10^{-13} to 3.5×10^{-18} cm^{-2}). The change in the activation energy was greater than could be accounted for by a band gap change due to interdiffusion (about 40 meV). Laurenço suggests that the change is directly associated with band bending at the CdTe grain boundaries, i.e. the valence band deformation is decreased by $CdCl_2$ treatment.

In order to study the influence of varying the nominal stoichiometry of the CdTe on cell parameters Chou [32] avoided the constraints of direct vapour methods by using MOCVD. Efficiency, V_{oc} and J_{sc} were reported as a function of the Te/Cd precursor ratio. A peak in performance was seen for Te/Cd = 6. The study implicates V_{Cd} as an important species for the control of conductivity. In the same work it was also noted that the degree of interdiffusion at the CdTe–CdS interface was maximised under conditions of excess Te. Some authors consider this interdiffusion to be responsible for the displacement of the electrical p–n junction away from the metallurgical interface and into the CdTe. Certainly this is the positioning revealed by EBIC experiments [41].

2.3. The CdTe/CdS interface

Interdiffusion at the CdTe/CdS interface is important not least due to its influence on optical absorption in the structure caused by the associated band gap changes. CdTe and CdS are not miscible in all proportions, as is shown in the pseudobinary equilibrium phase diagram in

Ohata's paper [42] and in subsequent work [43–46]. Nevertheless metastable samples of the entire composition range have been prepared and used to construct the band gap–composition diagram and a synthesis of data from a number of sources [42,47–49] is reported by Jensen [46] (see also Ref. [50]). Although addition of CdTe into CdS depresses the band gap from 2.42 eV as might be expected, the bowing is such that a band gap minimum is observed at $\sim$30% CdS. This minimum is about 0.1 eV lower than the band gap of pure CdTe. The effect of the interdiffusion of CdTe into CdS is to curtail the spectral response at its low λ end by reducing the window transmission. On the other hand incorporation of some CdS into the CdTe extends the spectral response to longer wavelengths. Both effects are clearly seen in Lee's work [26] and are widely reported. Reduction of the degree of diffusion of CdTe into CdS is generally considered to be desirable. Post-growth treatment of the CdS may assist by reducing the possibility of interdiffusion mediated by grain boundary migration and recrystallisation.

Given its importance an increasing number of physical studies of the interdiffusion are being undertaken by XRD, SIMS [16] and even spectroscopic STM [38].

It is suspected that the interdiffusion may be responsible for important electrical changes undergone by the cell during $CdCl_2$ processing. For example interdiffusion is associated with a decrease in the diode ideality factor, indicating a reduction in the interface state density [39].

Edwards [51] reports a study of the PL spectroscopy of a bevel etched CSS CdTe/CdS/TCO cell and an identical but CdS-free control structure (both had been $CdCl_2$ treated). Further results are presented here. In both samples the CdTe spectra (8 K) had an excitonic related peak and deeper, more intense luminescence at $\sim$1.48 eV attributed to complex D–A transitions. Changes in the intensity of this peak as a function of distance from the CdTe/substrate interface are shown in Fig. 4. The CdS containing sample shows a clear increase in $\sim$1.48 eV luminescence intensity within 3.5 μm of the CdTe/CdS interface. It is very likely that diffusion of S into CdTe can affect electrically important levels for some microns into the CdTe.

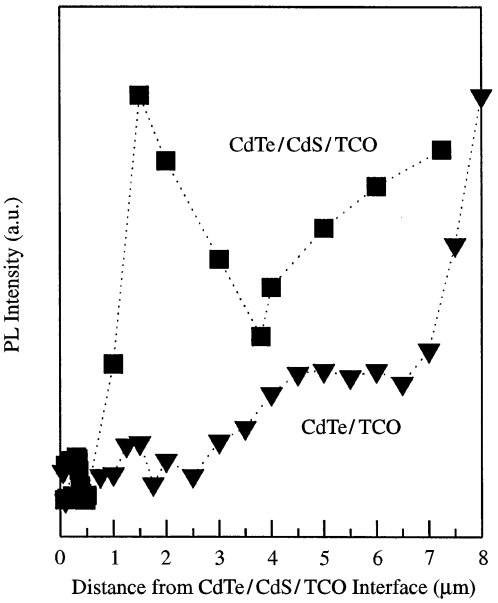

Fig. 4. Intensity of near band edge PL from CSS CdTe at 8 K (approx. 1.48 eV, 793 nm) for $CdCl_2$ treated CdTe/CdS/TCO and CdTe/TCO. Measurements are as a function of distance from the CdTe/(CdS or TCO) interface on bevelled samples. There is an increase in intensity of the PL from the CdTe/CdS sample near to the interface which is not present in the control sample.

2.4. 'Back contacts' to CdTe

Formation of low resistance back contacts to p-CdTe is the subject of much literature on account of the fundamental technical difficulty involved: CdTe has a high electron affinity ($\chi = 4.5$ eV) and no metal exists with a high enough work function (W_m) to give a zero Schottky barrier height given by $\Phi_b = (\chi + E_g) - W_m$. All contacts to p-CdTe therefore have a barrier which has the opposite sense to that of the p–n junction. The effect of this can be seen in the temperature dependent I–V curves for a CSS cell contacted with Au (Fig. 5). At room temperature the forward current is severely limited by the barrier. Analysis of similar curves using a two diode equivalent circuit analysis is described in Ref. [52]. Given that a back contact barrier is inevitable some consider that a barrier height of $<$200 meV will be acceptable for device operation.

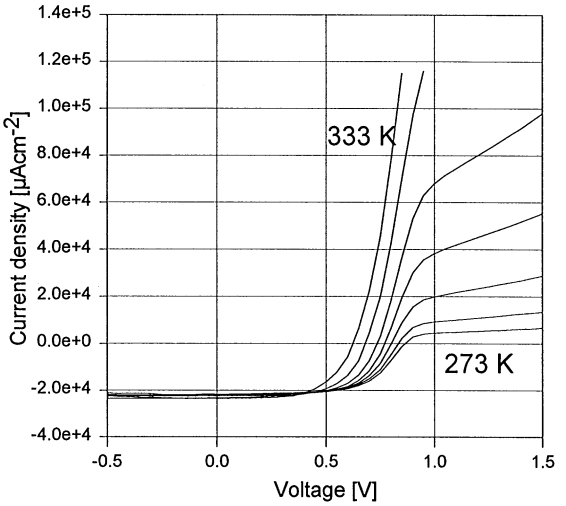

Fig. 5. Temperature dependence of the *I–V* curve between 273 and 373 K for a CSS Au/CdTe/CdS/TCO cell. The influence of the back contact barrier is evident in the 'roll over' of the forward bias response at lower temperatures.

Contacting to CdTe is reviewed by Fahrenbruch [53], Brinkman [54] and briefly by Birkmire [6]. The main strategies to overcome the barrier problem are (i) to use p^+ doping to reduce the barrier width or (ii) to use a p-type semiconductor as the back contact. p^+ doping has been effective with Cu, e.g. in ZnTe : Cu, but such contacts are unstable to Cu diffusion which eventually poisons the heterojunction. Use of a p-type contact material has been explored for the case of Te. Indeed Te-rich surfaces are often prepared by chemical etching prior to the deposition of other contact materials.

Although Te-rich surfaces can be prepared by etching with bromine/methanol and HNO_3/H_3PO_4 for example, the latter is preferred as it gives more reliable contacts [39]. Te-rich surfaces are susceptible to oxidation to TeO_2 [55] and some groups use a reducing agent prior to further treatment to eliminate it [56]. Oxidation of Te or of the CdTe itself beneath metallisations has been shown to be the mechanism of contact degredation via formation of an MIS structure [57].

Niles [58] reports a photoemission study of the Te/CdTe interface. The Te valence band minimum was found to be a function of the Te overlayer thickness. Minimisation of the Schottky barrier to about 0.26 eV could be achieved if Te were used which was thick enough to assume its native p-type conductivity; thinner layers were dominated by interface states and were n-type leading to higher barriers. Niles [58] also demonstrates that etching to make a Te-rich surface effects Te-enrichment deep within polycrystalline CdTe. After etching with HNO_3/H_3PO_4 XPS depth profiling showed significant Te enrichment to a depth of 1.2 μm compared to only 100 nm for single crystal material. Significantly Levi [18] shows that room temperature etching with this reagent, or bromine/methanol, or evaporation of Te leads directly to changes in the CdTe PL excited through the front wall of the cell. Levi's experiments were on 10 μm CdTe. AES mapping of the back wall CdTe after etching revealed that excess Te is concentrated at the grain boundaries. The reader is reminded of the crevasses at the grain boundaries and the potential for $CdCl_2$ to be present at those boundaries, as described in Section 2.2.

3. Some EBIC and cathodoluminescence observations of grain boundaries in CSS CdTe/CdS solar cells

3.1. EBIC

Electron beam induced currents (EBIC) generated by the beam of an SEM are a proven method of probing the spatial distribution of recombination centres due to defects. Its use to study grain boundaries in CdTe/CdS solar cells will be described briefly here. EBIC images are essentially maps of the short circuit current collected by the junction after carriers have been excited by the electron beam. The method is most often used to probe cleaved solar cells in the cross-section geometry to reveal the junction position. CdTe/CdS solar cells often show shallow homojunction behaviour [41]. However, to see grain boundaries the cell must be imaged in a planar geometry. Galloway [59] concludes that back wall images are difficult to interpret, but made the advance [41] of chemically removing the glass from the front wall, thus allowing front-wall EBIC for the first time. The images so obtained were beam current

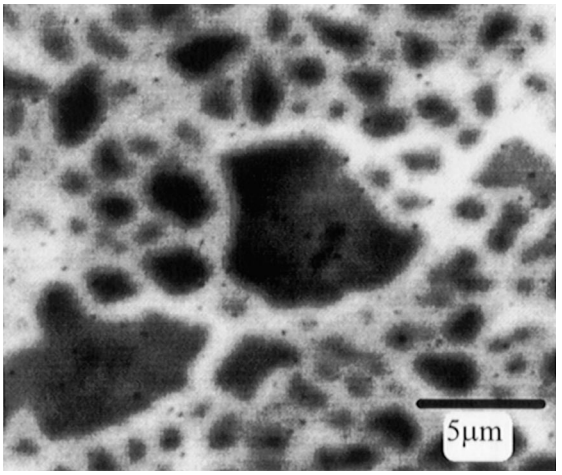

Fig. 6. SEM/EBIC image of a CdTe/CdS/TCO cell taken in a front-wall (glass off) planar geometry using a beam current of 0.5 nA. From Edwards et al. [51]. The injection density is many times higher than that due to solar irradiation and bright contrast at the grain boundaries has resulted, indicating better carrier collection under these conditions. Imaging under different injection levels has enabled the onset of high injection, and hence the effective majority carrier level to be mapped with high resolution [60].

dependent. At low beam currents giving generation comparable to solar irradiation rates there was virtually no contrast and grain boundaries could not be distinguished. This direct evidence of grain boundary passivation was only observed in $CdCl_2$ treated cells. At higher beam currents, where the injection levels exceeded those due to solar irradiation by some orders of magnitude, the unusual bright grain boundary contrast shown in Fig. 6 was seen. Bright contrast (representing enhanced carrier collection) appeared at a certain beam current threshold. The beam current dependence of the contrast effects was interpreted in terms of the onset of "high injection" conditions at the grains, before it is reached at the grain boundaries. High injection is said to prevail when the density of injected carriers exceeds that of the majority carriers responsible for the band bending at the p–n junction. Under such conditions electron hole pairs are collected less efficiently since the junction field is screened. For the case of bright grain boundary contrast (Fig. 6) the grains were considered to be at high injection (low collection) while the grain boundary regions – presumably on account of a higher local carrier concentration – were not. The experiment has been developed into a form of carrier density microscopy by Edwards [60], and is being further verified and developed.

Further analysis of the images of CdTe/CdS solar cells suggested a model for the band structure of grain boundaries which accounts for both the above results and the *dark* grain boundary images from earlier back wall EBIC experiments. All are consistent with there being upward band bending at the grain boundaries i.e. electron barriers. The repulsion of minority carriers which would result is consistent with grain boundary passivation.

3.2. Cathodoluminescence microscopy

Limited cathodoluminescence microscopy has been undertaken on polished back walls of fully processed CSS solar cells [41]. Monochromatic imaging of the exciton related and D–A luminescent bands at 117 K is shown in Fig. 7. While the excitonic luminescence is clearly much reduced at grain boundaries, the spatial distribution of D–A centres is more diffuse. Close inspection of the images reveals that in general the D–A luminescence is weakest in the centres of large grains and strongest at some grain boundaries or groups of small grains. This observation is consistent with the luminescence being associate with species diffusing from grain boundary locations.

4. Conclusions

Research in CdTe/CdS solar cells has been driven by the desire to demonstrate the highest possible conversion efficiencies for the materials system. Many investigations have been empirical but have nevertheless resulted in a technology which is now being industrialised in its existing form. The same polycrystalline character of the material which makes it attractive for cheap production is also responsible for many of the technical difficulties. Many of the processing steps have inter-related influences upon critical cell parameters. Diffusion and its acceleration by grain boundaries, and the $CdCl_2$ treatment are very influential.

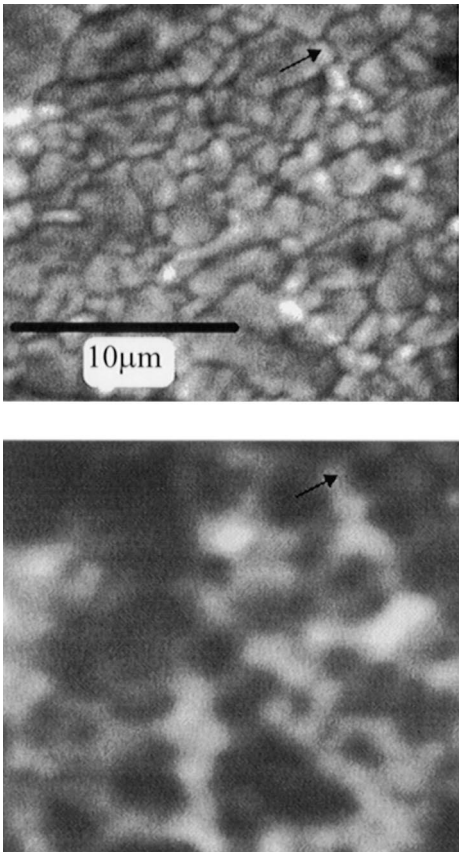

Fig. 7. Monochromatic SEM cathodoluminescence images of a polished CdTe surface of a CSS CdTe/CdS/TCO cell, taken at 117 K. The exposed surface is 3.0 ± 0.08 μm above the CdTe/CdS interface. The upper image shows how excitonic luminescence (1.576 eV, 785 nm) originates from the grains but is quenched at the boundaries. The lower is a map of luminescent bands centred on 860 nm (1.439 eV). This D–A luminescence originates from some grain boundaries and small grains. The marker indicates a grain. From Galloway et al. [41].

Current research effort is aimed at the next generation of production solar cells. Indeed the stability of the CdTe/CdS cell in the market will depend on advances in key areas such as:-

(1) Understanding of the CdTe doping and $CdCl_2$ processing,

(2) Interface and grain boundary passivation effects,

(3) Developments of stable contacts with low barriers,

(4) Understanding of how different parts of the cell influence one-another (e.g. the influence of the back contact on the junction).

Although this understanding is desirable for the future, the current technology is nevertheless viable: the CdTe/CdS cell and its processing represent a very fortunate combination of complex but compatible materials behaviours.

Acknowledgements

The authors would like to thank ANTEC GmbH, Simon Galloway at Oxford Instruments and M. Laurenço, K.P. Homeward and Wai Lek Ng of UNN and Surrey.

References

[1] N. Zanio, Cadmium telluride, in: R.K. Willardson, A.C. Beer (Eds.), Semiconductors and Semimetals, vol. 13, Wiley, New York, 1978.
[2] D. Bonnet, H. Rabenhorst, in: 9th IEEE Photovoltaic Specialists Conf., IEEE, Silver Springs, MD, 1972, p. 219.
[3] A.L. Farhenbruch, R.H. Bube, Fundamentals of Solar Cells, Photovoltaic Solar Energy Conversion, Academic Press, New York, 1983.
[4] A.E. Rakhshani, J. Appl. Phys. 81 (12) (1997) 7988.
[5] T.H. Myers, S.W. Edwards, J.F. Schetzina, J. Appl. Phys. 52 (6) (1981) 4231.
[6] R.W. Birkmire, E. Eser, Annu. Rev. Mater. Sci. 27 (1997) 625.
[7] J. Britt, C. Ferekides, Appl. Phys. Lett. 62 (22) (1993) 2851.
[8] T. Aramoto, S. Kumusawa, Jpn. J. Appl. Phys. 36 (1997) 6304.
[9] Y.Y. Loginov, K. Durose, H.M. Al-Allak, S.A. Galloway, S. Oktik, A.W. Brinkman, H. Richter, D. Bonnet, J. Crystal Growth 163 (1995) 159.
[10] B. Basol, S. Ou, O. Statsudd, J. Appl. Phys. 58 (10) (1985) 3809.
[11] H.M. Al-Allak, A.W. Brinkman, H. Richter, D. Bonnet, J. Crystal Growth 159 (1996) 910.
[12] S.A. Ringel, A.W. Smith, M.H. MacDougal, A. Rohatgi, J. Appl. Phys. 70 (2) (1991) 881.
[13] H.R. Moutinho, F.S. Hasoon, L.L. Kazmerski, Progr. Photovoltaics 3 (1) (1995) 39.
[14] H.R. Moutinho, M.M. Al-Jassim, F.A. Abulfotuh, D.H. Levi, P.C. Dippo, R.G. Dhere, L.L. Kazmerski, in: 26th IEEE Photovoltaic Specialists Conf., Anaheim, 1997, p. 431.
[15] B. Qi, D. Kim, D.L. Williamson, J.U. Trefny, J. Electrochem. Soc. 143 (2) (1996) 517.

[16] R.G. Dhere, S.E. Asher, K.M. Jones, M.M. Al-Jassim, H.R. Moutinho, D.H. Rose, P. Dippo, P. Sheldon, AIP Conf. Proc. 353 (1) (1996) 392.
[17] A. De Vos, J.E. Parrot, P. Baruch, P.T. Landsberg, in: 14th European Photovoltaic Solar Energy Conf., Amsterdam, 1994, p. 1315.
[18] D.H. Levi, L.M. Woods, D.S. Albin, T.A. Gessert, D.W. Niles, A. Swartzlander, D.H. Rose, R.K. Ahrenkiel, P. Sheldon, in: 26th PVSC, IEEE, Anaheim, CA, 1997, p. 351.
[19] P.F. Gerhardinger, R.J. McCurdy, Mater. Res. Soc. Symp. Proc. 426 (1996) 399.
[20] K.W. Mitchell, C. Eberspacher, F. Cohen, J. Avery, G. Duran, W. Bottenberg, Solar Cells 23 (1988) 49.
[21] D. Bonnet, in: 14th PVSEC, WIP, Barcelona, 1997.
[22] I. Kaur, D.K. Pandya, K.L. Chopra, J. Electrochem. Soc. 127 (4) (1980) 943.
[23] M.E. Ozsan, in: 1st WCPEC, IEEE, Hawaii, 1994, p. 327.
[24] M.E. Ozsan, in: 13th Eurpean PVEC, Nice, 1995, p. 2115.
[25] A. Kylner, E. Niemi, in: 13th European PVSEC, WIP, Barcelona, 1997, p. 1326.
[26] J.S. Lee, H.B. Im, J. Mater. Sci. 21 (1986) 980.
[27] N. Romeo, A. Bosio, R. Tedeschi, V. Romeo, D. Cavevari, D. Leone, in: 14th European PVSEC, H.S. Stephens and Associates, Barcelona, 1997, p. 2351.
[28] D.W. Niles, D. Rioux, H. Hochst, J. Appl. Phys. 73 (9) (1993) 4586.
[29] Z.C. Feng, H.C. Chou, A. Rohatgi, G.K. Lim, A.T.S. Wee, K.L. Tan, J. Appl. Phys. 79 (4) (1996) 2151.
[30] R.W. Clemminck, M. Burgleman, M. Casteleyn, B. Depuydt, Int. J. Solar Eng. 12 (1992) 67.
[31] M.P.R. Panicker, M. Knaster, F.A. Kroger, J. Electrochem. Soc. 125 (4) (1978) 567.
[32] H.C. Chou, A. Rohatgi, N.M. Jokerst, S. Kamra, S.R. Stock, S.L. Lowrie, R.K. Ahrenkiel, D.H. Levi, Mater. Chem. Phys. 43 (2) (1996) 178.
[33] T. Taguchi, J. Shirafuji, Y. Inuishi, Jpn. J. Appl. Phys. 13 (7) (1974) 1169.
[34] F. Humphreys, M. Hatherly, Recrystallisation and Related Annealing Phenomena, 1st ed., Pergamon Press, Oxford, 1995.
[35] D. Kim, B. Qi, D.L. Williamson, J.U. Trefny, in: First WCPEC, IEEE, Hawaii, 1994, p. 338.
[36] J. Saraie, M. Kitagawa, M. Ishida, T. Tanaka, J. Crystal Growth 43 (1978) 13.
[37] I.K. Andronik, P. Kuleva, K. Suschkevich, Inorg. Mater. 12 (1976) 759.
[38] D.H. Levi, H.R. Moutinho, F.S. Hasoon, B.M. Keyes, R.K. Ahrenkiel, M. Aljassim, L.L. Kazmerski, R.W. Birkmire, Solar Energy Mater. Solar Cells 41 (2) (1996) 381.
[39] A. Rohatgi, R. Sudharsanan, S.A. Ringel, M.H. MacDougal, Solar Cells 30 (1991) 109.
[40] M. Laurenço, W.L. Ng, K.P. Homewood, K. Durose, Phys. Rev. Lett. (1998), submitted.
[41] S.A. Galloway, P.R. Edwards, K. Durose, Inst. Phys. Conf. Ser. 157 (1997) 579.
[42] K. Ohata, J. Saraie, T. Tanaka, Jpn. J. Appl. Phys. 12 (1973) 1798.
[43] S.-Y. Nunoue, T. Hemmi, E. Kato, J. Electrochem. Soc. 137 (4) (1990) 1248.
[44] D.G. Moon, H.B. Im, Powder Metall. 35 (1) (1992) 53.
[45] I. Clemminck, M. Burgelman, M. Caseleyn, J. De Poorter, A. Vervaet, in: 22nd IEEE Photovoltaic Specialists Conf., IEEE, Las Vegas, Nevada, 1991, p. 1114.
[46] D.G. Jensen, B.E. McCandless, R.W. Birkmire, Proc. Mater. Res. Soc. Symp. 426 (1996) 325.
[47] D. Bonnet, Phys. Stat. Sol. (a) 3 (1970) 913.
[48] R. Hill, D. Richardson, Thin Solid Films 18 (1973) 25.
[49] S.K. Al-Ani, M.N. Makadsi, K. Al-Shakarchi, C.A. Hogarth, J. Mater. Sci. 28 (1993) 251.
[50] R. Radojcic, A. Hill, M.J. Hamphsire, Solar Cells 4 (1981) 101.
[51] P.R. Edwards, D.P. Halliday, K. Durose, H. Richter, D. Bonnet, in: 14th Photovoltaic Solar Energy Conf., WIP, Barcelona, 1997, p. 2083.
[52] G. Stollwerck, J.R. Sites, in: 13th European PVEC, WIP, Nice, 1995.
[53] A.L. Fahrenbruch, Solar Cells 21 (1987) 399.
[54] A.W. Brinkman, in: P. Capper (Ed.), Properties of Narrow Gap Cadmium Based Compounds, IEE, Stevenage, 1994, p. 575.
[55] F.A. Ponce, R. Sinclair, R.H. Bube, Appl. Phys. Lett. 39 (12) (1981) 951.
[56] S. Oktik, M.E. Ozsan, M.H. Patterson, Patent WO 93/09568, World Intellectual Property Organisation, International Bureau, B.P. Solar Limited, 13 May 1993.
[57] T.L. Chu, S.S. Chu, S.T. Ang, J. Appl. Phys. 58 (8) (1985) 3206.
[58] D.W. Niles, X. Li, P. Sheldon, J. Appl. Phys. 77 (9) (1995) 4489.
[59] S.A. Galloway, K. Durose, Inst. Phys. Conf. Ser. 146 (1995) 709.
[60] P.R. Edwards, K. Durose, S.A. Galloway, D. Bonnet, H. Richter. in: Proc. Mater. Congress '98, IoM, Cirencester, 1998.
[61] G.S. Oleinik, P.A. Mizetskii, T.P. Nuzhnaya, Inorg. Mater. 22 (1) (1986) 164.